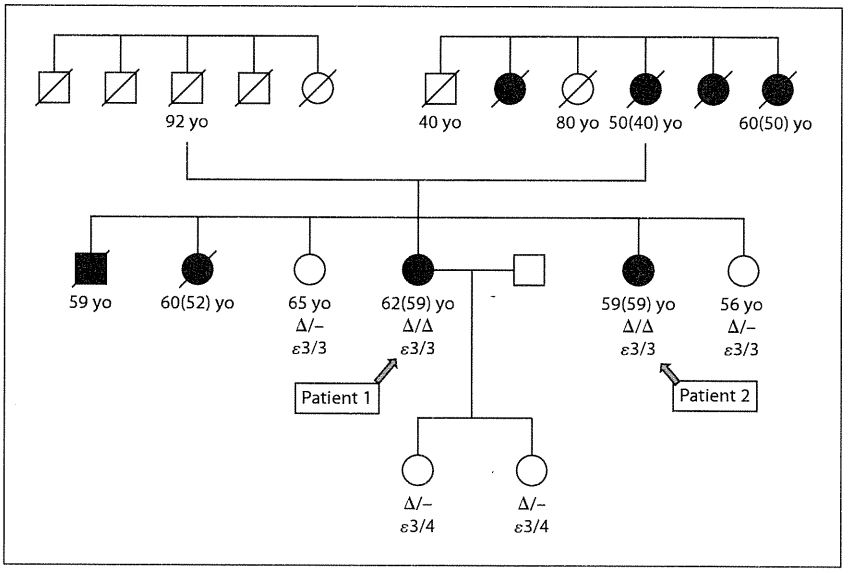

Fig. 1. Pedigree chart of the family carrying the E693Δ mutation. The numbers indicate the ages of the family members at the time of death, at the time of the investigation of the gene, or at the time of the onset of the disease. The Δ denotes the deletion of E693. The affected patients were homozygous for this mutation. The ε denotes the Apo E genotype. yo = Years old.

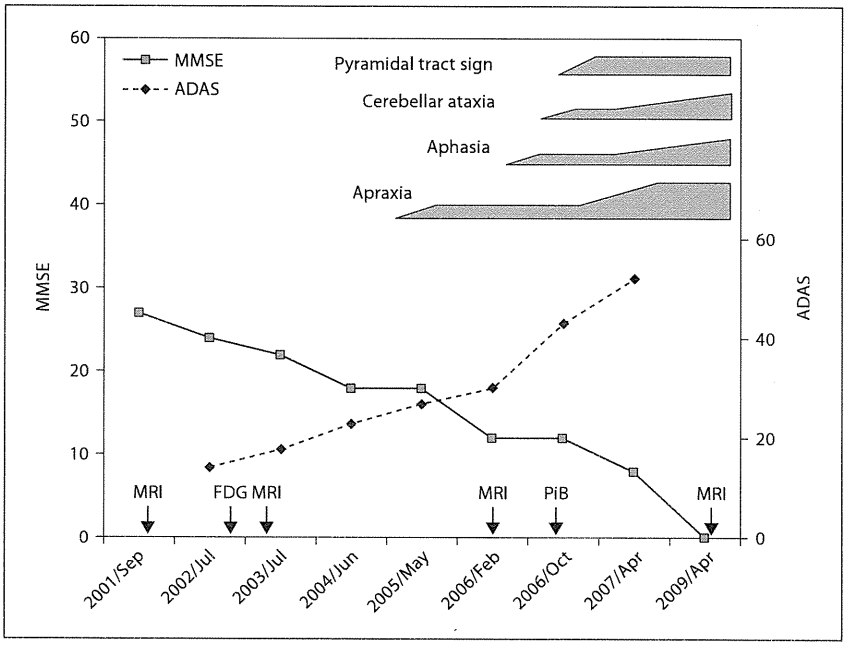

Fig. 2. Chart of the clinical course of patient 1. MMSE scores are graphed against the Alzheimer's Disease Assessment Scale (ADAS) scores. After the patient was diagnosed with mild cognitive impairment, her cognitive level declined gradually. Three years later, the patient developed apraxia and gait disturbance due to ataxia.

tional Institute of Neurological and Communicative Disorders and Stroke-AD and Related Disorders Association (NINCDS-ADRDA) criteria, she was diagnosed with AD, and treatment with donepezil was started.

Two years later, she showed dramatic changes in her clinical symptoms at the age of 61. Her MMSE score decreased to 12. She developed cerebellar ataxia, gait disturbances, apraxia, positive signs of pyramidal tract disturbances, including hyperreflexia of the patellar and Achilles tendons, and a positive sign of pathological reflex and spasticity in the lower extremities, none of which had been observed before. These features are unusual for patients with AD.

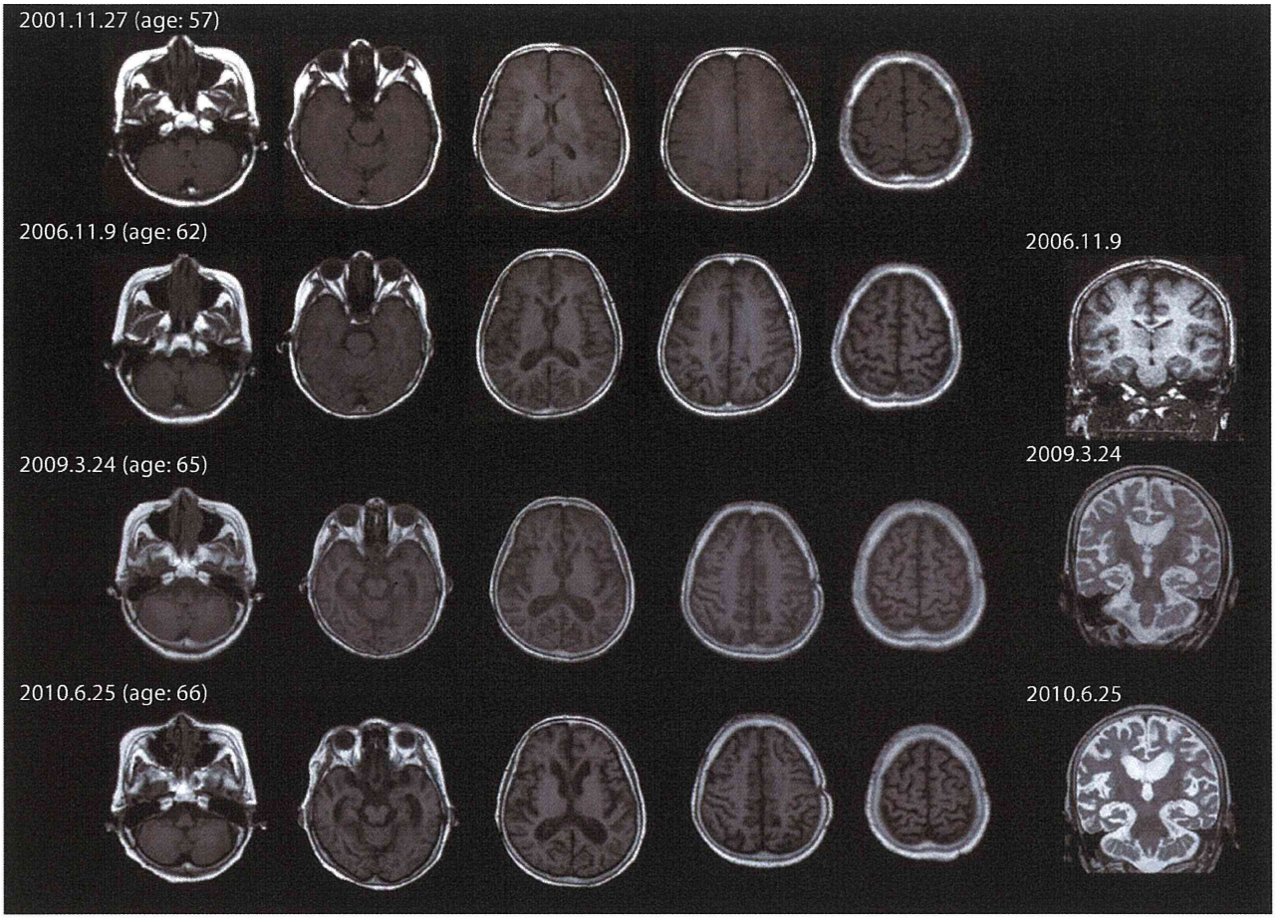

Fig. 3. MRI scans for patient 1 at the ages of 57, 62, 65, and 66. At the first visit, the MRI scans revealed no atrophy of the hippocampus. At the mid-stage of the disease (when the patient was 62), MRI images revealed slight worsening of the atrophy. After the patient entered the apallic state, atrophies of the hippocampus and the cerebral cortex were evident, but atrophy of the cerebellum was not detected.

Her cognitive impairment became very severe at the age of 62 when she had an MMSE score of 5. Nevertheless, an MRI scan revealed only mild parietal lobe atrophy (fig. 3) and no significant atrophy in the hippocampus. In addition, a [^{11}C]PiB-PET scan revealed almost no amyloid accumulation in the cortex (fig. 4b). An FDG-PET scan showed decreased glucose metabolism throughout the brain of patient 1 except in the motor and sensory cortices and in the cerebellum (fig. 4c). At the age of 63, she became unable to walk by herself, and she fell in her house several times. After a chronic subdural hemorrhage due to a fall, she became bedridden, and her cognitive dysfunction worsened.

At the age of 65, her general status was comparable to that of a patient with apallic syndrome. MRI scans revealed moderate atrophy of the hippocampus, mild atrophy of the cerebrum, and mild dilatation of the third and lateral ventricles (fig. 3). It is noteworthy that, despite the severity of her cognitive dysfunction, only mild atrophy was detected in the cerebrum, which is in contrast to patients with sporadic AD who usually show severe atrophy in this region. CSF biomarker levels of Aβ and tau were highly indicative of AD. For instance, her CSF levels of Aβ1–42 and Aβ1–40 were 4.1 and 242.8 pg/ml, respectively, which were very low compared with published values in the US AD Neuroimaging Initiative study [15] and in a Japanese cohort study [16]. Moreover, the levels of

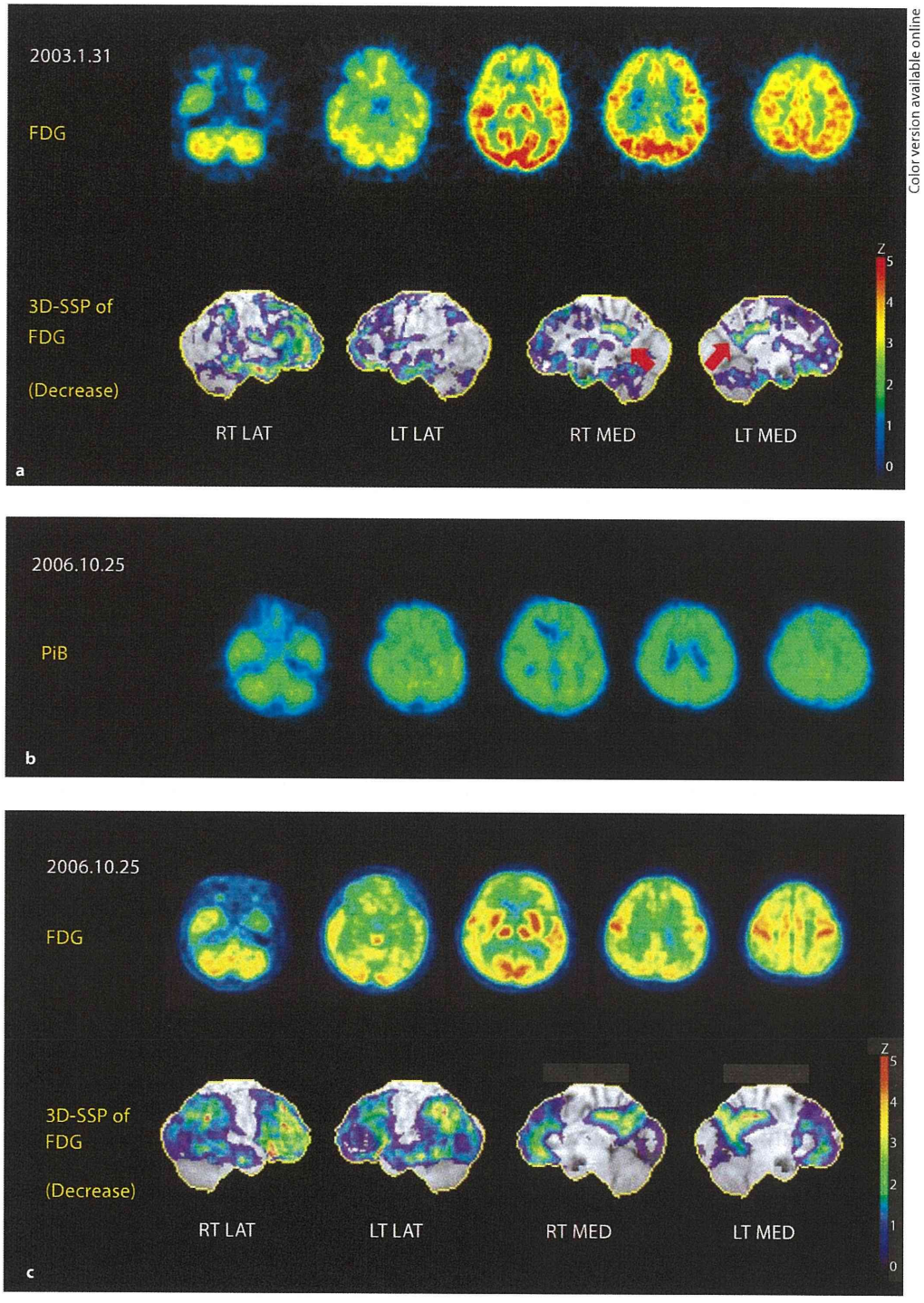

Color version available online

Fig. 4. a FDG and the 3D-SSP analysis of patient 1 showed FDG hypometabolism in the posterior cingulate cortex, which was similar to that seen in patients with sporadic AD (arrow). **b** PiB-PET images of patient 1. No accumulation of amyloid is seen in her brain. **c** FDG and 3D-SSP analysis images of patient 1, 3 years later than those in **a**. 3D-SSP reveals decreased glucose metabolism throughout the patient's brain, except in the motor and sensory cortices and in the cerebellum.

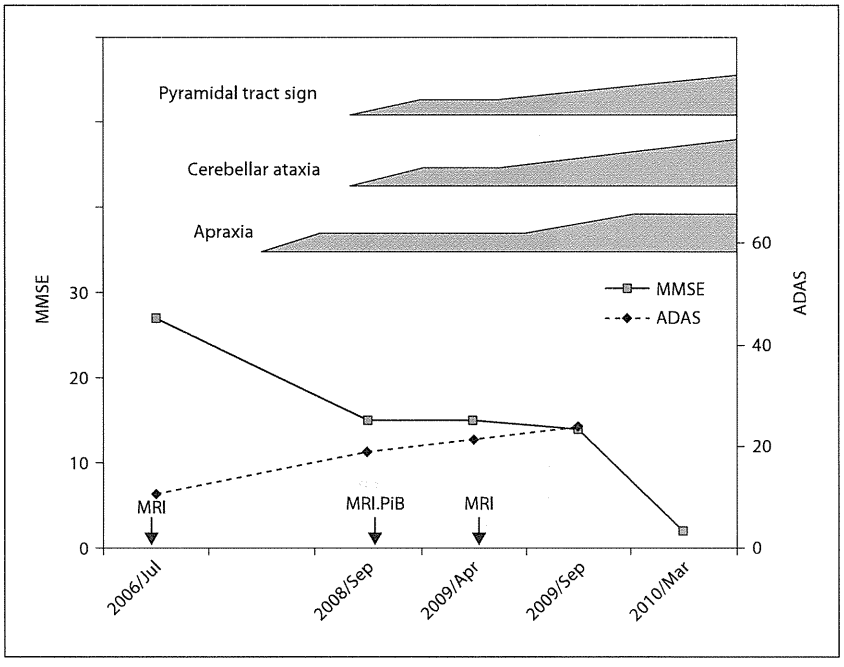

Fig. 5. Chart of the clinical course of patient 2. MMSE scores are graphed against the Alzheimer's Disease Assessment Scale (ADAS) scores. After the patient developed cerebellar ataxia, apraxia, and positive signs of pyramidal tract disturbances, her cognitive level declined rapidly.

total tau and phosphorylated tau in her CSF were 628 and 87.2 pg/ml, respectively (normal values in our institute: tau, <400 pg/ml; p-tau, <75 pg/ml). These values alone suggest that patient 1 was in an advanced phase of AD.

Patient 2

Patient 2 was the younger sister of patient 1 (fig. 1). She was carefully followed because she had homozygous alleles of the Osaka (E693Δ) mutation. When we found her homozygous mutation, she was 55. At that time, she was very thoughtful and polite to us and did not show any mental or behavioral abnormalities.

She experienced memory disturbances at the age of 59 and, hence, underwent a checkup at our hospital. However, her MMSE was 27 at that time. After that, her memory gradually worsened, and she was prescribed donepezil by her home doctor half a year later. Her condition worsened, and she again visited our hospital at the age of 61. She could speak fluently, but her MMSE score was 15 (fig. 5). A domain-specific cognitive evaluation was performed. Her recent memory was decreased to a score of 1 on the CCMT, 3 on the Pict-1, and 4 on the Pict-2 (table 1). The patient's visuospatial function showed mild to moderate decline, and her scores on the CDT and BDT decreased to 9 and 10, respectively. Her answer on the CDT showed distortion of the hour-hand of the clock, and both hands were the same length. She showed an apparent decrease of her executive function with the results of 113 s on the TMT-A, and she was unable to do the TMT-B. The category fluency test showed relative preservation, and she could name 13 vegetables and 11 animals in a minute. She had a mild depressive mood with a score of 7 on the Geriatric Depression Scale. Her naming ability was relatively preserved with a score of 16 out of 17 on the RBMT naming subtest. These results suggest that her cognitive decline was compatible with moderate AD due to the obvious abnormalities in her recent memory and her general cognitive decline without predominant decline in executive and visuospatial functions. Similar to patient 1, she exhibited cerebellar ataxia, gait disturbances, and signs of disturbances in the pyramidal tract at the age of 61. An MRI scan revealed only mild cortical atrophy (fig. 6). A [^{11}C]PiB-PET scan revealed no amyloid accumulation in the cerebral cortex (fig. 7). These clinical features were very similar to those of patient 1. The levels of Aβ1–42 and Aβ1–40 in her CSF were 9.5 and 285.2 pg/ml, respectively, and those of total tau and phosphorylated tau were 856 and 152 pg/ml, respectively. Again, these values alone suggested that patient 2 was in an advanced phase of AD similar to patient 1. At the age of 62, she could barely walk, even with the assistance of her family, and her MMSE score was 12.

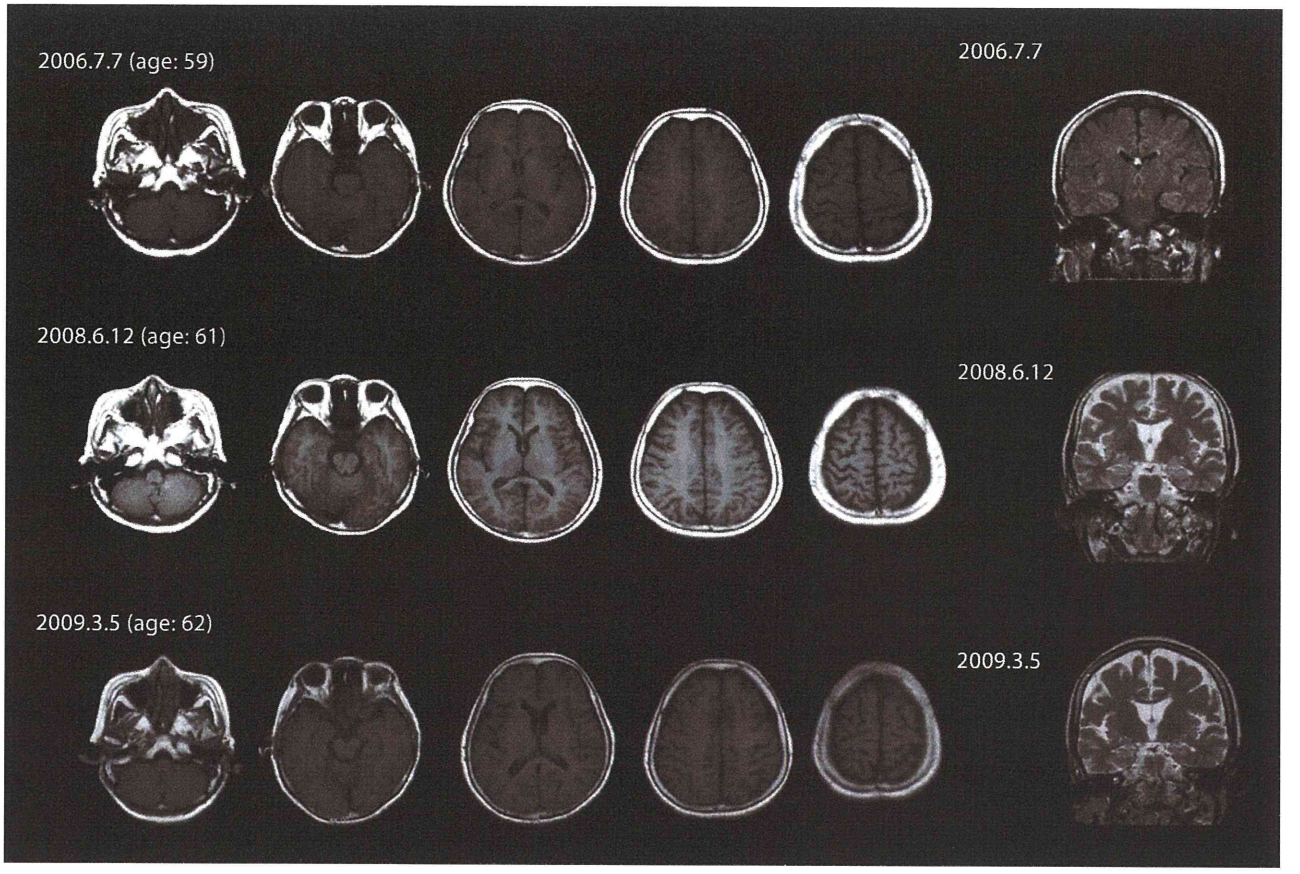

Fig. 6. MRI of patient 2 at the ages of 59, 61, and 62. The first MRI scan showed no atrophy of the brain. After her cognition decreased, her MRI images revealed slight cortical atrophy and no atrophy of the hippocampus.

Table 1. Neuropsychological evaluation in patient 2

Cognitive function	Test	Her score/maximum	Normal range
	MMSE	15/30	≥24
Recent memory	CCMT	1/16	≥9
	Pict-1	3/23	≥12
	Pict-2	4/23	≥15
Visuospatial function	CDT	9/10	≥10
	BDT	10/61	≥31
Attention, executive function	Category fluency (vegetable)	13	≥11
	Category fluency (animal	11	≥11
	Letter fluency ('ka')	7	≥11
	TMT-A	113	≤43
	TMT-B	NA	
Depressive state assessment	Geriatric Depression Scale	7	<5

The data suggest that the patient developed memory disturbances and a loss of visuospatial function and executive function similar to that seen in patients with sporadic AD.

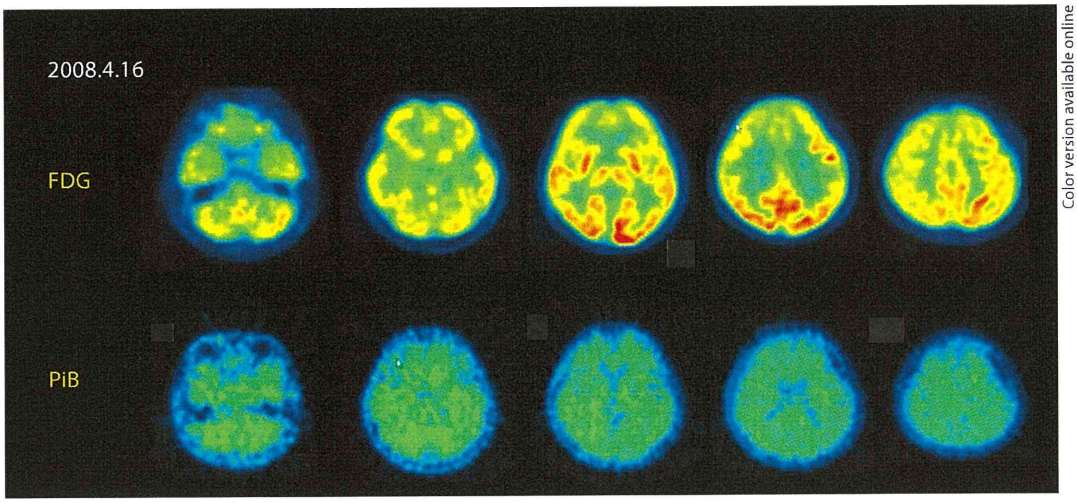

Color version available online

Fig. 7. FDG- and PiB-PET images of patient 2. PiB-PET images show no accumulation of amyloid in her brain, similar to that seen in patient 1.

Discussion

We report here on 2 cases who were sisters in the same pedigree, who were both carrying an APP E693Δ mutation, and who possessed the same genotype of apolipoprotein E (ε3/3ε3). Both of these cases had a variant type of AD. They developed very similar symptoms and showed a similar progression of the disease. In the early stages of the disease, they exhibited only memory disturbances, but they soon lost their visuospatial cognitive and executive functions. However, neither evident brain atrophy nor evident amyloid deposition was seen in the cortex. In the late stages, these patients displayed mild to moderate brain atrophy and unexpected motor dysfunction. These clinical features are unique and distinctive compared to patients with typical AD in several aspects.

First, our patients showed an apparent discrepancy between their cognitive impairment and apparent brain atrophy on MRI images. They first exhibited memory disturbances without any distinct atrophy. Similar observations were unexpectedly limited from our experiences in patients with AD when we considered their clinical dementia scales. The 3D-SSP analysis of the FDG-PET of patient 1 showed glucose hypometabolism in the posterior cingulate cortex, which is similar to that seen in patients with sporadic AD at the very early stages. This means that the mechanisms underlying the neuronal damage caused by the oligomers mimicked what happens in sporadic AD patients, and it caused the AD-like symptoms of these patients in their early stages. After the early stage, the rate of memory disturbance progression in these patients was apparently faster than that seen in sporadic AD cases. However, at this stage, brain atrophy was not apparent.

In our opinion, we speculate that both the memory disturbances and the subsequent brain atrophy were caused by Aβ oligomers due to synaptic failure, but the resulting neuronal death required a longer period of time of cellular exposure to the Aβ oligomers. Compared with typical AD, we expect that our patients possess higher levels of Aβ oligomers in their brains, and they therefore exhibited memory disturbances at earlier ages. However, since the Aβ oligomer-induced neurodegeneration required a long time, brain atrophy occurred only in the late stages. The second 3D-SSP analysis of FDG-PET of patient 1 showed severe hypoglucose metabolism throughout the brain except in the motor and sensory cortices and cerebellum, even though she could not walk due to cerebellar ataxia. In typical AD, the concentrations of brain Aβ oligomers increase gradually, and neurons are exposed to Aβ oligomers for a long time before the disease onset, which leads to eventual neurodegeneration. Once Aβ oligomers reach a certain level, patients display memory disturbances, and in the clinic, their brain atrophy is observed simultaneously. However, we cannot exclude the possibility that amyloid fibrils, rather than Aβ oligomers, primarily contribute to brain atrophy, and, thus, our patients did not possess significant

atrophy due to their lack of amyloid fibril formation. In addition, the formation of neurofibrillary tangles as another late pathology may contribute to atrophy, as is evident in most dementia-like frontotemporal dementia, tangle dementia, and argyrophilic grain dementia. In either case, our findings clearly suggest that neurodegeneration does not correlate with cognitive decline, which reflects synaptic failure and which was probably caused by pathological Aβ oligomers [1]. This notion might be confirmed by a new method of imaging that detects Aβ oligomers and/or dysfunctional synapses.

Another unique point of our patients is the appearance of motor dysfunction. Typical sporadic AD rarely shows cerebellar ataxia and signs of pyramidal tract disturbances. Patients bearing presenilin-1 (PS-1) mutations exhibited spasticity of their legs, but they did not exhibit cerebellar ataxia [17]. Patients with spinocerebellar ataxia (SCA) showed not only spasticity and cerebellar ataxia, but also dementia [18–22]. In this regard, the clinical features of our patients were similar to those of SCA patients. The major difference between our patients and those with SCA is that SCA patients usually exhibit atrophy of the cerebellum in conjunction with the inability to walk, but our patients exhibited no apparent atrophy or hypoglucose metabolism of the cerebellum when they could not walk. The present ataxia in our patients may be caused by synaptotoxicity of Aβ oligomers that accumulated in the cerebellum and ataxia. This notion may be in part supported by the observation that PiB-retention signals were slightly detected in the cerebellum of our patients (fig. 4b, 7), since amyloid-binding dyes, including PiB, have been shown to recognize Aβ oligomers as well as amyloid fibrils. We speculate that the metabolism of Aβ oligomers and the vulnerability of neurons to Aβ oligomers in the cerebellum may be different from those in the cerebrum; Aβ oligomers could be cleared more efficiently and neurons are less vulnerable to Aβ oligomers in the cerebellum. Therefore, motor dysfunction associated with cerebellar ataxia is rarely observed in typical AD, whereas our patients, with higher levels of Aβ oligomers, exhibited these symptoms after a long period of time.

Recently, we reported on a novel mouse model of AD expressing the Osaka (E693Δ) mutation [23]. This transgenic mouse displayed an age-dependent intraneuronal accumulation of Aβ oligomers from 8 months of age but no extracellular amyloid deposits, even at 24 months. Aβ accumulation was detected not only in the cerebral cortex and hippocampus but also in the cerebellum. Their hippocampal-related synaptic plasticity and memory functions were impaired at 8 months, and the levels of the presynaptic marker synaptophysin in the hippocampus began to decrease with the same timing. Furthermore, abnormal tau phosphorylation was detected from 8 months, and neuronal loss in the hippocampus was observed at 24 months. These findings seem to support our speculation concerning the underlying mechanisms of the disease process in our patients described above. The CSF levels of Aβ1–42 in our patients were significantly lower than those in patients with typical AD, and CSF levels of total and phosphorylated tau were as high as those seen in patients with typical AD. These results suggest that Aβ accumulated in the brain parenchyma, possibly within neurons, and the pathological changes related to tau occurred in our patients, similar to that seen in our mouse model.

Lastly, it is a new and difficult challenge to distinguish clinical symptoms in AD that are caused by Aβ oligomers versus amyloid fibrils because of their simultaneous occurrence in the brain. Our patients, however, are presumed to possess only Aβ oligomers in their brains. Thus, the symptoms of our patients presented here are expected to reflect pathological functions of Aβ oligomers. Our findings suggest that Aβ oligomers primarily cause cognitive dysfunction in the early stages of the disease and, in some cases, elicit motor dysfunction through cerebellar ataxia in the late stages. Aβ oligomers can induce neurodegeneration that leads to brain atrophy, but it requires a long period of time of neuronal exposure to Aβ oligomers. We also found that brain atrophy does not correlate with cognitive impairment. Finally, we suggest that senile plaques are a less important target, but we acknowledge the practical view that plaques are currently a useful marker of disease progression. Thus, the pathological significance of senile plaque formation remains to be further studied in AD.

Acknowledgment

This study was supported by the Ministry of Education, Culture, Sports, Science and Technology (MEXT) of Japan (Grants-in-Aid for Scientific Research 21613007). This study was also supported by Grants-in-Aid for Comprehensive Research on Dementia from the Ministry of Health, Labour and Welfare, Japan; and in part by the Alzheimer's Association (IIRG-09-132098).

Disclosure Statement

Competing interests: none. Patient consent: obtained.

References

1 Selkoe DJ: Alzheimer's disease is a synaptic failure. Science 2002;298:789–791.
2 Cleary JP, Walsh DM, Hofmeister JJ, Shankar GM, Kuskowski MA, Selkoe DJ, Ashe KH: Natural oligomers of the amyloid-beta protein specifically disrupt cognitive function. Nat Neurosci 2005;8:79–84.
3 Lesne S, Koh MT, Kotilinek L, Kayed R, Glabe CG, Yang A, Gallagher M, Ashe KH: A specific amyloid-beta protein assembly in the brain impairs memory. Nature 2006;440:352–357.
4 Lacor PN, Buniel MC, Furlow PW, Clemente AS, Velasco PT, Wood M, Viola KL, Klein WL: Abeta oligomer-induced aberrations in synapse composition, shape, and density provide a molecular basis for loss of connectivity in Alzheimer's disease. J Neurosci 2007;27:796–807.
5 Shankar GM, Bloodgood BL, Townsend M, Walsh DM, Selkoe DJ, Sabatini BL: Natural oligomers of the Alzheimer amyloid-beta protein induce reversible synapse loss by modulating an NMDA-type glutamate receptor-dependent signaling pathway. J Neurosci 2007;27:2866–2875.
6 Nimmrich V, Ebert U: Is Alzheimer's disease a result of presynaptic failure? Synaptic dysfunctions induced by oligomeric beta-amyloid. Rev Neurosci 2009;20:1–12.
7 Tomiyama T, Nagata T, Shimada H, Teraoka R, Fukushima A, Kanemitsu H, Takuma H, Kuwano R, Imagawa M, Ataka S, Wada Y, Yoshioka E, Nishizaki T, Watanabe Y, Mori H: A new amyloid beta variant favoring oligomerization in Alzheimer's-type dementia. Ann Neurol 2008;63:377–387.
8 Lopresti BJ, Klunk WE, Mathis CA, Hoge JA, Ziolko SK, Lu X, Meltzer CC, Schimmel K, Tsopelas ND, DeKosky ST, Price JC: Simplified quantification of Pittsburgh Compound B amyloid imaging PET studies: a comparative analysis. J Nucl Med 2005;46:1959–1972.
9 Price JC, Klunk WE, Lopresti BJ, Lu X, Hoge JA, Ziolko SK, Holt DP, Meltzer CC, DeKosky ST, Mathis CA: Kinetic modeling of amyloid binding in humans using PET imaging and Pittsburgh Compound-B. J Cereb Blood Flow Metab 2005;25:1528–1547.
10 Rouleau I, Salmon DP, Butters N, Kennedy C, McGuire K: Quantitative and qualitative analyses of clock drawings in Alzheimer's and Huntington's disease. Brain Cogn 1992;18:70–87.
11 Funabiki Y, Takechi H, Akamatsu T, Kita T: Development of a short neuropsychological battery to screen early dementia in the elderly. Geriatr Gerontol Int 2003;2:179–186.
12 Lezak MD: Neuropsychological Assessment, ed 3. New York, Oxford University Press, 1995.
13 Takechi H, Dodge HH: Scenery Picture Memory Test: a new type of quick and effective screening test to detect early stage Alzheimer's disease patients. Geriatr Gerontol Int 2010;10:183–190.
14 Minoshima S, Frey KA, Koeppe RA, Foster NL, Kuhl DE: A diagnostic approach in Alzheimer's disease using three-dimensional stereotactic surface projections of fluorine-18-FDG PET. J Nucl Med 1995;36:1238–1248.
15 Vemuri P, Wiste HJ, Weigand SD, Shaw LM, Trojanowski JQ, Weiner MW, Knopman DS, Petersen RC, Jack CR Jr: MRI and CSF biomarkers in normal, MCI, and AD subjects: diagnostic discrimination and cognitive correlations. Neurology 2009;73:287–293.
16 Shoji M, Matsubara E, Murakami T, Manabe Y, Abe K, Kanai M, Ikeda M, Tomidokoro Y, Shizuka M, Watanabe M, Amari M, Ishiguro K, Kawarabayashi T, Harigaya Y, Okamoto K, Nishimura T, Nakamura Y, Takeda M, Urakami K, Adachi Y, Nakashima K, Arai H, Sasaki H, Kanemaru K, Yamanouchi H, Yoshida Y, Ichise K, Tanaka K, Hamamoto M, Yamamoto H, Matsubayashi T, Yoshida H, Toji H, Nakamura S, Hirai S: Cerebrospinal fluid tau in dementia disorders: a large scale multicenter study by a Japanese study group. Neurobiol Aging 2002;23:363–370.
17 Ataka S, Tomiyama T, Takuma H, Yamashita T, Shimada H, Tsutada T, Kawabata K, Mori H, Miki T: A novel presenilin-1 mutation (Leu85Pro) in early-onset Alzheimer disease with spastic paraparesis. Arch Neurol 2004;61:1773–1776.
18 Twells R, Yenchitsomanus PT, Sirinavin C, Allotey R, Poungvarin N, Viriyavejakul A, Cemal C, Weber J, Farrall M, Rodprasert P, et al: Autosomal dominant cerebellar ataxia with dementia: evidence for a fourth disease locus. Hum Mol Genet 1994;3:177–180.
19 Oyanagi S: Hereditary dentatorubral-pallidoluysian atrophy. Neuropathology 2000;20(suppl):S42–S46.
20 Filla A, De Michele G, Cocozza S, Patrignani A, Volpe G, Castaldo I, Ruggiero G, Bonavita V, Masters C, Casari G, Bruni A: Early onset autosomal dominant dementia with ataxia, extrapyramidal features, and epilepsy. Neurology 2002;58:922–928.
21 Rolfs A, Koeppen AH, Bauer I, Bauer P, Buhlmann S, Topka H, Schols L, Riess O: Clinical features and neuropathology of autosomal dominant spinocerebellar ataxia (sca17). Ann Neurol 2003;54:367–375.
22 Vale J, Bugalho P, Silveira I, Sequeiros J, Guimarães J, Coutinho P: Autosomal dominant cerebellar ataxia: frequency analysis and clinical characterization of 45 families from Portugal. Eur J Neurol 2010;17:124–128.
23 Tomiyama T, Matsuyama S, Iso H, Umeda T, Takuma H, Ohnishi K, Ishibashi K, Teraoka R, Sakama N, Yamashita T, Nishitsuji K, Ito K, Shimada H, Lambert MP, Klein WL, Mori H: A mouse model of amyloid beta oligomers: their contribution to synaptic alteration, abnormal tau phosphorylation, glial activation, and neuronal loss in vivo. J Neurosci 2010;30:4845–4856.

Journal of Geriatric Psychiatry
and Neurology
24(3) 123-126
© The Author(s) 2011
Reprints and permission:
sagepub.com/journalsPermissions.nav
DOI: 10.1177/0891988711409410
http://jgpn.sagepub.com
SAGE

Pittsburgh Compound B-Negative Dementia—A Possibility of Misdiagnosis of Patients With Non-Alzheimer Disease-Type Dementia as Having AD

Hiroyuki Shimada, MD[1], Suzuka Ataka, MD[1], Jun Takeuchi, MD[1], Hiroshi Mori, PhD[2], Yasuhiro Wada, PhD[3], Yasuyoshi Watanabe, MD[3,4], and Takami Miki, MD[1]

Abstract

Amyloid imaging has been used to detect amyloid deposition in the brain. We performed Pittsburgh compound B (PiB)-positron emission tomography on 63 patients with dementia having cognitive decline or memory disturbance. In addition, we measured the patients' apolipoprotein E4 (apo E4) status and cerebrospinal fluid (CSF) levels of amyloid-β (Aβ)1-42, tau, and P-tau. Finally, the patients were diagnosed as having probable Alzheimer disease (AD) on the basis of their neuropsychological findings and because they met the National Institute of Neurological and Communicative Disorders and Stroke and the Alzheimer's Disease and Related Disorders Association criteria. Among the patients diagnosed with probable AD, 10 patients were PiB negative. The CSF levels of P-tau and tau in PiB-negative patients were significantly lower than those in the PiB-positive patients. In addition, the CSF levels of Aβ1-42 in the PiB-negative patients were significantly higher than those in the PiB-positive patients. None of the PiB-negative patients were apo E4 carriers. These results suggest that the PiB-negative patient group included not only AD patients but also non-AD-type dementia patients. However, our finding is based on a relatively small number of patients and therefore should be replicated in a larger cohort. In addition, it will be necessary to categorize these participants by longitudinal follow-up and postmortem pathological examinations.

Keywords

PiB-PET, PiB-negative dementia, CSF biomarkers, non-AD type dementia

Received October 8, 2010. Received revised March 14, 2011. Accepted for publication March 15, 2011.

Introduction

The neuropathological features of Alzheimer disease (AD) include the formation of extracellular senile plaques and intraneuronal neurofibrillary tangles. Amyloid-β (Aβ) protein is a major component of these senile plaques. Klunk et al reported that ^{11}C-labeled Pittsburgh compound B ([^{11}C]-PiB) has a high affinity for Aβ, and [^{11}C]-PiB has been used as an amyloid-imaging compound since their report was published.[1] ^{11}C-labeled Pittsburgh compound B-positron emission tomography (PET) has shown amyloid deposition in patients with AD and in some patients with mild cognitive impairment (MCI).[2] Furthermore, PiB does not bind to the neurofibrillary tangles or brain homogenates that are not associated with plaques.[3] In previous studies on non-AD-type dementia, PET did not show an increased [^{11}C]-PiB uptake.[4]

Among the patients clinically diagnosed with AD, some were PiB negative. In this study, we evaluated the cerebrospinal fluid (CSF) levels of biomarkers and the status of apolipoprotein E (apo E) in PiB-negative patients (PiB-negative dementia group). We compared the results of this study with those obtained from the studies on PiB-positive patients with AD.

[1] Department of Geriatrics and Neurology, Osaka City University Graduate School of Medicine, Osaka, Japan
[2] Department of Neuroscience, Osaka City University Graduate School of Medicine, Osaka, Japan
[3] RIKEN Center for Molecular Imaging Science, Kobe, Japan
[4] Department of Physiology, Osaka City University Graduate School of Medicine, Osaka, Japan

Corresponding Author:
Hiroyuki Shimada, Department of Geriatrics and Neurology, Osaka City University Graduate School of Medicine, 1-4-3 Asahimachi, Abeno-ku, Osaka 545-8585, Japan
Email: h.shimada@med.osaka-cu.ac.jp

Table 1. The Demographic Characteristics and the Levels of Biomarkers in the Cerebrospinal Fluid (CSF) of Pittsburgh Compound B (PiB)-Positive and PiB-Negative Patients[a]

	PiB (+) AD	PiB (−) AD	*P* Value
N	21	10	
Gender	5 M, 16 F	5 M, 5 F	
Age	74.8 ± 3.1	77.3 ± 4.8	
Mean Mini-Mental State Examination (MMSE) score	22.5 ± 3.5	23.9 ± 2.5	
Pittsburgh compound B (PiB) mean cortical distribution–volume ratio (MCDVR)	1.56 ± 0.26	0.99 ± 0.15	.001
Cerebrospinal fluid (CSF) amyloid β (Aβ1-42; pg/mL)	385.7 ± 107.1	559.6 ± 243.3	.05
CSF P-tau (pg/mL)	107.1 ± 37.8	68.4 ± 46.7	.05
CSF total tau (pg/mL)	580.4 ± 222.6	277.9 ± 220	.01
Apolipoprotein E (apo E) E4 carriers (%)	13 (62%)	0	.001

[a] Table demographic data of Pittsburgh compound B (PiB)-positive and PiB-negative patients and the levels of biomarkers in their cerebrospinal fluid. The analysis was performed on only 21 of the 53 PiB-positive patients and on 10 PiB-negative patients.

Methods

Participants

We recruited 63 patients with AD from the Department of Geriatrics and Neurology, Osaka City University Hospital. These patients met the criteria for probable AD as defined by the National Institute of Neurological and Communicative Disorders and Stroke and the Alzheimer's Disease and Related Disorders Association (NINCDS-ADRDA). Informed consent was obtained from all patients or their next of kin. This study was approved by the Ethics Committee of Osaka City University Graduate School of Medicine.

Positron Emission Tomography

We synthesized [^{11}C]-PiB using 2-(4′-aminophenyl)-6-hydroxybenzothiazole as the labeled precursor molecule. After an intravenous injection of [^{11}C]-PiB (150-300 MBq), we performed a 60-minute, dynamic, 3-dimensional list-mode emission scan without arterial sampling using an Eminence-B PET scanner (Shimadzu Corporation, Kyoto, Japan).

Magnetic resonance imaging (MRI) scans were aligned with corresponding PET images using the PMOD Image Fusion Tool (PMOD Technologies Ltd, Zurich, Switzerland). These images were reconstructed using a filtered back-projection algorithm with attenuation and scatter corrections. We used the Logan graphical analysis method to calculate each regional count (distribution–volume ratio [DVR]) with the cerebellum as a reference and using the frame summation of dynamic images for 40 to 60 minutes.[5] We selected the cortical regions in the frontal, parietal, precuneus, posterior cingulate, and lateral temporal lobes. The mean cortical DVR (MCDVR) is the mean of the DVR values in these regions. We defined the cutoff level of the MCDVR as 1.3, which was based on the distribution of DVR values of normal controls and patients who were diagnosed with PiB positive by visual inspection. Patients were judged to be PiB positive based on visual inspection by a single reader or if the MCDVR and DVR values obtained from at least 3 main cortical areas were higher than 1.3 each. The patients were judged to be PiB negative if they showed no or low PiB retention in most cortical areas and if the MCDVR values were lower than 1.3.

Biomarkers

The CSF samples were obtained from the L3/L4 or L4/L5 interspaces in the morning and were collected in 10-mL polypropylene tubes. The CSF samples were aliquoted into 0.5- or 1-mL polypropylene tubes and stored at −80°C until further analysis. We measured the levels of Aβ1-42 in the CSF using an enzyme-linked immunosorbent assay (ELISA) kit (Wako Pure Chemical Industries Ltd, Japan). We measured the levels of tau and P-tau 181 in the CSF using a sandwich ELISA kit (Innotest; Innogenetics, Belgium).

Statistical Analysis

Statistical analysis was performed using the commercially available software (SPSS, version 16.0 for Windows; SPSS Inc, Chicago, Illinois). Nonparametric tests were used because the variables were not normally distributed. Mann-Whitney test was used to compare the demographics of the patients in PiB-positive and PiB-negative groups.

Results

In this study, we observed that the levels of [^{11}C]-PiB uptake in 10 of the 63 patients with dementia who were clinically diagnosed with AD were as low as those in normal patients. These PiB-negative patients included 4 men and 6 women (mean age, 73.3 ± 7.4 years). We observed no differences between the PiB-negative and PiB-positive patients with AD (19 men and 34 women; mean age, 70.2 ± 8.3 years) with respect to clinical presentation, particularly in their neuropsychological features, including memory disturbances, visuospatial cognition, and executive function. The patients met the NINCDS-ADRDA criteria. We assessed the differences between the levels of CSF biomarkers and apo E status in 10 PiB-negative patients and the first 21 of the 53 PiB-positive patients who agreed to undergo the examination. The CSF levels of tau and P-tau in the PiB-negative patients were significantly lower than those in the

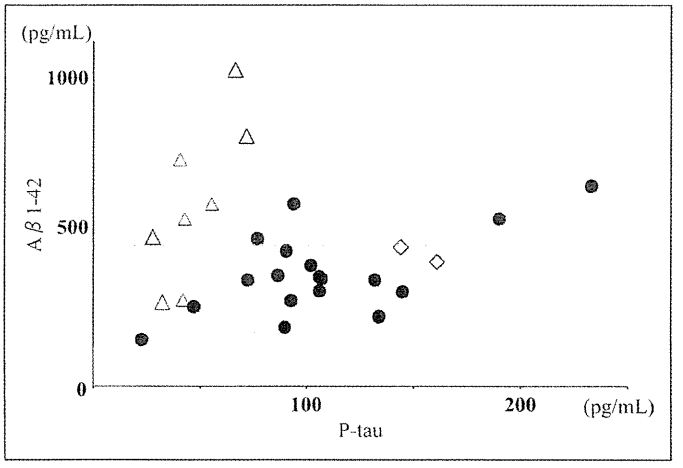

Figure 1. The closed circles (●) represent the Pittsburgh compound B (PiB)-positive patients. The other symbols (Δ, ◇) represent the PiB-negative patients. The lines indicate cutoff values in our laboratory.

PiB-positive patients, and the CSF levels of Aβ1-42 in the PiB-negative patients were significantly higher than those in the PiB-positive patients (Table 1). None of the PiB-negative patients was a carrier for the apo E4 genotype (Table 1). The CSF levels of P-tau in 8 of the 10 PiB-negative patients were within normal ranges and were lower than those in most PiB-positive patients (Figure 1, open triangles). Among the 8 PiB-negative patients, 6 were negative for each Aβ1-42, P-tau, and apo E4. Two patients had low CSF Aβ1-42 levels and normal P-tau levels, and 2 patients had high P-tau and Aβ1-42 levels that were just below the cutoff level (Figure 1, open diamonds). The 4 PiB-positive patients had normal Aβ1-42 levels.

Discussion

Our results indicate that low levels of Aβ deposition were observed in the neocortex of some patients clinically diagnosed with probable AD. We propose that, in these patients, the dementia can be referred to as PiB-negative dementia. This entity may include sporadic AD, familial AD, and other types of dementia such as dementia with Lewy bodies (DLB), frontotemporal dementia (FTD), argyrophilic grain dementia (AGD), neurofibrillary tangle-predominant dementia (NFTPD), and hippocampal sclerosis. In our study, 6 PiB-negative patients were negative for Aβ1-42, P-tau, and apo E4. These patients were considered to have a pathological background different from that of the patients with AD, as described above. Since 2 PiB-negative patients had low Aβ1-42 and normal P-tau levels, we assumed that the CSF Aβ1-42 levels might have been lowered before an increase in PiB retention.

Two previous reports have shown that 2 patients diagnosed with sporadic AD on the basis of autopsy findings were PiB negative.[6,7] However, the Cairns case had a diagnosis of possible AD or low-probability AD because of the low densities of neuritic plaques and tangles. Rosen et al only performed a postmortem study and did not investigate in vivo PiB levels.

In our case, 2 cases, 2 PiB-negative patients, were diagnosed with AD because of the high levels of P-tau and low levels of Aβ1-42 in their CSF. Furthermore, we assumed that several other cases of PiB-negative dementia may be AD. These 2 cases indicate that PiB retention may be less sensitive than CSF Aβ1-42 levels. We had previously reported that patients with familial AD, who had a low tendency for Aβ aggregation, showed negative PiB staining.[8] In addition, we would like to emphasize that among the PiB-positive patients, 4 had normal Aβ1-42 levels, suggesting that PiB retention can increase before Aβ1-42 levels drop below the cutoff value.

Because some PiB-negative patients showed low CSF levels of P-tau and high CSF levels of Aβ1-42, these patients were thought to be non-AD-type patients with dementia. In our study, all PiB-negative patients showed AD-like neuropsychological characteristics; these patients showed no behavioral abnormalities like those in patients with FTD, and none of them met the diagnostic criteria for probable DLB.[9] In addition, it is difficult to differentiate between FTD or DLB and early-stage AD.[10] Previous reports have shown that the clinical features of AGD[11,12] and NFTPD[13,14] are indistinguishable from those of AD. In some cases, these diseases are characterized by gradually progressing dementia with prominent memory disturbances and considerable preservation of other cognitive functions. Therefore, we speculate that patients with non-AD-type dementia may be misdiagnosed as having AD, and some of the patients with non-AD-type dementia may have been included in our PiB-negative patient group.

It is necessary to consider several limitations of our study. First, the total number of patients with dementia was only 63, which is too small to determine the rate of PiB-negative patients in patients clinically diagnosed with AD. Further studies should be performed with a larger number of patients with dementia using the PiB-PET method. Second, we did not perform postmortem analyses and were therefore unable to confirm the diagnosis in these PiB-negative patients with dementia. Third, we evaluated our patients only by MRI and by the CSF biomarkers in this report. There are several other examinations that are used for the evaluation of patients with dementia, including fluorodeoxyglucose (FDG)-PET, volumetric MRI analysis, single photon emission tomography, and other neuropsychological evaluations.

In conclusion, our findings show that the PiB-negative patient group with dementia included patients with non-AD-type dementia; and in clinics and hospitals where PiB-PET cannot be performed, PiB-negative patients with dementia were misdiagnosed as having early-stage AD. Pittsburgh compound B-negative dementia should be accounted for when developing an anti-amyloid treatment of AD.[15] Further clinical studies are required to completely understand the pathological characteristics of such PiB-negative patients with dementia.

Acknowledgment

We would like to thank Dr Hajime Takechi (Kyoto University, Geriatrics) for performing excellent neuropsychological examinations of our patients.

Declaration of Conflicting Interests

The authors declared no conflicts of interest with respect to the authorship and/or publication of this article.

Funding

The authors disclosed receipt of the following financial support for the research and/or authorship of this article: by the Ministry of Education, Culture, Sports, Science and Technology (MEXT) of Japan (Grant-in-aid for Scientific Research 21613007).

References

1. Klunk WE, Engler H, Nordberg A, et al. Imaging brain amyloid in Alzheimer's disease with Pittsburgh Compound-B. *Ann Neurol.* 2004;55(3):306-319.
2. Kemppainen NM, Aalto S, Wilson IA, et al. PET amyloid ligand [11C]PIB uptake is increased in mild cognitive impairment. *Neurology.* 2007;68(19):1603-1606.
3. Klunk WE, Wang Y, Huang GF, et al. The binding of 2-(4'-methylaminophenyl)benzothiazole to postmortem brain homogenates is dominated by the amyloid component. *J Neurosci.* 2003; 23(6):2086-2092.
4. Rowe CC, Ng S, Ackermann U, et al. Imaging beta-amyloid burden in aging and dementia. *Neurology.* 2007;68(20):1718-1725.
5. Lopresti BJ, Klunk WE, Mathis CA, et al. Simplified quantification of Pittsburgh Compound B amyloid imaging PET studies: a comparative analysis. *J Nucl Med.* 2005;46(12):1959-1972.
6. Cairns NJ, Ikonomovic MD, Benzinger T, et al. Absence of Pittsburgh compound B detection of cerebral amyloid beta in a patient with clinical, cognitive, and cerebrospinal fluid markers of Alzheimer disease: a case report. *Arch Neurol.* 2009; 66(12):1557-1562.
7. Rosen RF, Ciliax BJ, Wingo TS, et al. Deficient high-affinity binding of Pittsburgh compound B in a case of Alzheimer's disease. *Acta Neuropathol.* 2009;119(2):221-233.
8. Tomiyama T, Nagata T, Shimada H, et al. A new amyloid mu variant favoring oligomerization in Alzheimer's-type dementia. *Ann Neurol.* 2008;63(3):377-387.
9. McKeith IG, Dickson DW, Lowe J, et al. Diagnosis and management of dementia with Lewy bodies: third report of the DLB Consortium. *Neurology.* 2005;65(12):1863-1872.
10. Piguet O, Halliday GM, Creasey H, Broe GA, Kril JJ. Frontotemporal dementia and dementia with Lewy bodies in a case-control study of Alzheimer's disease. *Int Psychogeriatr.* 2009;21(4):688-695.
11. Steuerwald GM, Baumann TP, Taylor KI, et al. Clinical characteristics of dementia associated with argyrophilic grain disease. *Dement Geriatr Cogn Disord.* 2007;24(3):229-234.
12. Togo T, Isojima D, Akatsu H, et al. Clinical features of argyrophilic grain disease: a retrospective survey of cases with neuropsychiatric symptoms. *Am J Geriatr Psychiatry.* 2005; 13(12):1083-1091.
13. Bancher C, Jellinger KA. Neurofibrillary tangle predominant form of senile dementia of Alzheimer type: a rare subtype in very old subjects. *Acta Neuropathol.* 1994;88(6):565-570.
14. Jellinger KA, Attems J. Neurofibrillary tangle-predominant dementia: comparison with classical Alzheimer disease. *Acta Neuropathol.* 2007;113(2):107-117.
15. Holmes C, Boche D, Wilkinson D, et al. Long-term effects of Abeta42 immunisation in Alzheimer's disease: follow-up of a randomised, placebo-controlled phase I trial. *Lancet.* 2008; 372(9634):216-223.

SAGE-Hindawi Access to Research
International Journal of Alzheimer's Disease
Volume 2011, Article ID 431320, 8 pages
doi:10.4061/2011/431320

Research Article

E22Δ Mutation in Amyloid β-Protein Promotes β-Sheet Transformation, Radical Production, and Synaptotoxicity, But Not Neurotoxicity

Takayuki Suzuki,[1] Kazuma Murakami,[1] Naotaka Izuo,[2] Toshiaki Kume,[2] Akinori Akaike,[2] Tetsu Nagata,[3] Tomoyuki Nishizaki,[3] Takami Tomiyama,[4] Hiroshi Takuma,[4] Hiroshi Mori,[4] and Kazuhiro Irie[1]

[1] *Laboratory of Organic Chemistry in Life Science, Division of Food Science and Biotechnology, Graduate School of Agriculture, Kyoto University, Sakyo-ku, Kyoto 606-8502, Japan*
[2] *Department of Pharmacology, Graduate School of Pharmaceutical Sciences, Kyoto University, Sakyo-ku, Kyoto 606-8501, Japan*
[3] *Department of Physiology, Hyogo College of Medicine, Nishinomiya 663-8501, Japan*
[4] *Department of Neuroscience, Graduate School of Medicine, Osaka City University, Osaka 545-8585, Japan*

Correspondence should be addressed to Kazuhiro Irie, irie@kais.kyoto-u.ac.jp

Received 16 October 2010; Accepted 16 November 2010

Academic Editor: Katsuhiko Yanagisawa

Copyright © 2011 Takayuki Suzuki et al. This is an open access article distributed under the Creative Commons Attribution License, which permits unrestricted use, distribution, and reproduction in any medium, provided the original work is properly cited.

Oligomers of 40- or 42-mer amyloid β-protein (Aβ40, Aβ42) cause cognitive decline and synaptic dysfunction in Alzheimer's disease. We proposed the importance of a turn at Glu22 and Asp23 of Aβ42 to induce its neurotoxicity through the formation of radicals. Recently, a novel deletion mutant at Glu22 (E22Δ) of Aβ42 was reported to accelerate oligomerization and synaptotoxicity. To investigate this mechanism, the effects of the E22Δ mutation in Aβ42 and Aβ40 on the transformation of β-sheets, radical production, and neurotoxicity were examined. Both mutants promoted β-sheet transformation and the formation of radicals, while their neurotoxicity was negative. In contrast, E22P-Aβ42 with a turn at Glu22 and Asp23 exhibited potent neurotoxicity along with the ability to form radicals and potent synaptotoxicity. These data suggest that conformational change in E22Δ-Aβ is similar to that in E22P-Aβ42 but not the same, since E22Δ-Aβ42 exhibited no cytotoxicity, unlike E22P-Aβ42 and wild-type Aβ42.

1. Introduction

Alzheimer's disease (AD) is characterized by amyloid deposition in senile plaques that are mainly composed of 40- and 42-mer amyloid β-proteins (Aβ40 and Aβ42) [1, 2]. These proteins are secreted from amyloid precursor protein (APP) by two proteases, β- and γ-secretases [3]. Aβ42 plays a more critical role in the pathogenesis of AD than Aβ40 because of its stronger aggregative ability and neurotoxicity [3]. Oxidative stress is believed to contribute to neuronal loss in AD [4–6]; one of the proposed mechanisms of Aβ42-induced neurotoxicity is related to the radicalization at both Tyr10 and Met35 accompanied by the generation of hydrogen peroxide [7, 8]. On the other hand, soluble oligomeric assembly of Aβ causes cognitive impairment and synaptic dysfunction in AD [9, 10].

Our previous investigation using solid-state NMR together with systematic proline replacement proposed a toxic conformer with a turn at positions 22 and 23 in Aβ42 aggregates and a nontoxic conformer with a turn at positions 25 and 26; the former showed a potent ability to aggregate, form oligomers, and exhibit neurotoxicity [11]. The turn formation at positions 22 and 23 along with the neighboring β-sheet structure in the toxic conformer of Aβ42 brought Tyr10 and Met35 close together to generate the *S*-oxidized radical cation at Met35, the ultimate toxic radical species, through oxidation by the phenoxy radical at Tyr10 produced by redox reactions [7, 12]. The mutations of Aβ are concentrated at

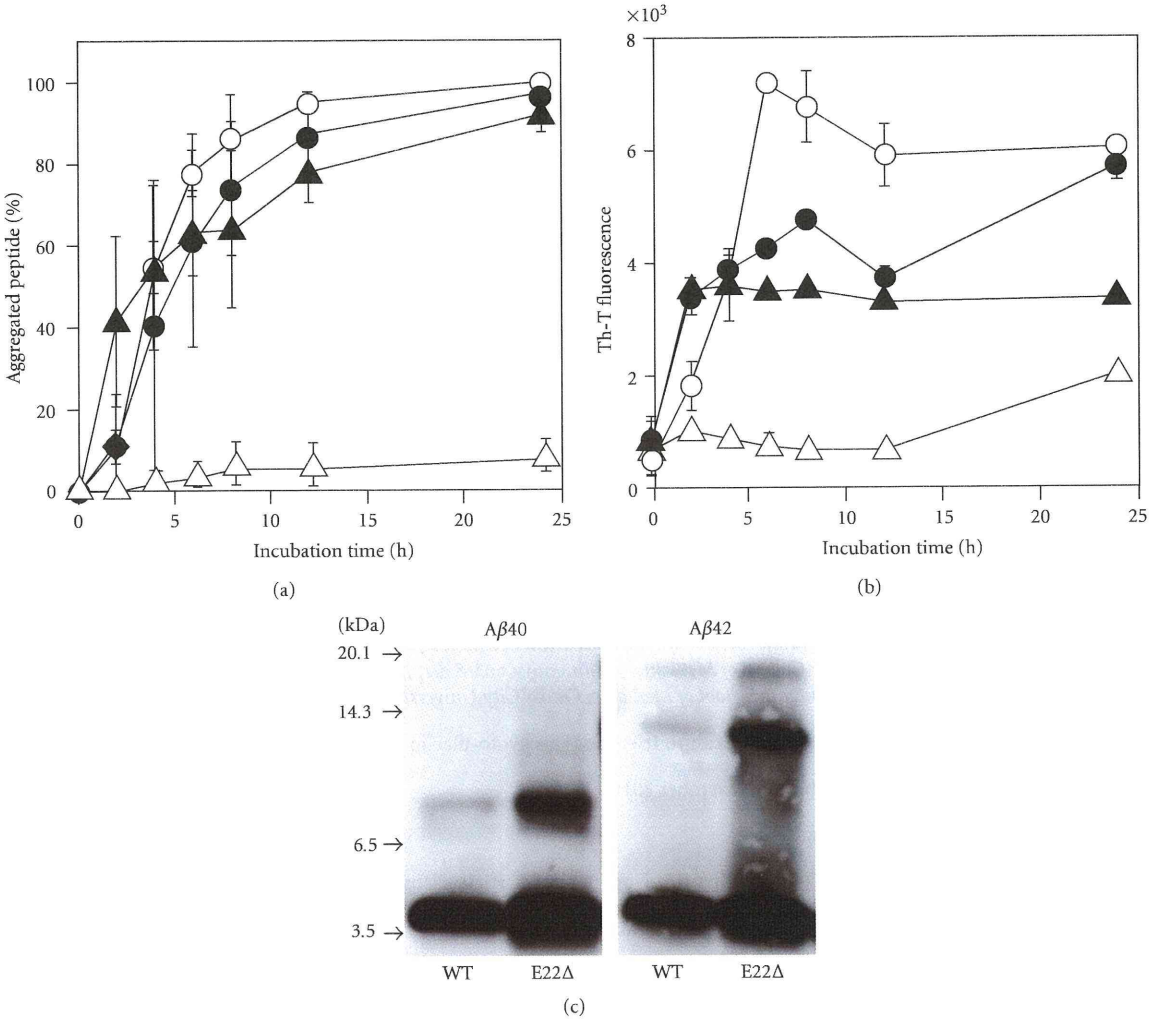

FIGURE 1: Aggregation profiles of E22Δ-Aβ40 and E22Δ-Aβ42 (25 μM) after incubation at 37°C. (a) Sedimentation assay estimated by HPLC analysis after centrifugation. (b) Th-T fluorescence assay. ○, Aβ42; △, Aβ40; ●, E22Δ-Aβ42; ▲, E22Δ-Aβ40. (c) Western blotting without incubation.

positions 21, 22, and 23; A21G (Flemish), E22G (Arctic), E22Q (Dutch), E22K (Italian), and D23N (Iowa) types. These mutations may play a pathological role in cerebral amyloid angiopathy (CAA) or familial AD (FAD) because these mutant proteins induced neuronal death *in vitro* more potently than wild-type Aβ42 [13]. Thus, Glu22 and Asp23 in Aβ are considered to be key residues for neurotoxicity through the formation of radicals.

Recently, Mori and coworkers reported that a novel mutation, in which the Glu-22 residue is defective (E22Δ), induced AD-type dementia without amyloid deposition, and that *in vitro* E22Δ-Aβ42 favorably formed low-molecular weight oligomers to inhibit long-term potentiation (LTP) compared with Aβ42 [14] and to induce synaptic alteration [15]. Therefore, the effects of the deletion at Glu22 on the secondary structure, formation of radicals, and neurotoxicity are interesting from the standpoint of discussing the role of the Glu-22 residue of Aβ42 in the pathogenesis of AD.

This paper describes a comprehensive study of the aggregative ability, secondary structure, radical-generating activity, neurotoxicity in primary rat cortical neuronal cell cultures, and the inhibitory activity of LTP of both E22Δ-Aβ40 and E22Δ-Aβ42. These results were compared with those of E22P-Aβ42 with a turn at positions 22 and 23.

2. Materials and Methods

2.1. Preparation of E22Δ-Aβ. E22Δ-Aβ40 and E22Δ-Aβ42 were synthesized by the method reported previously [16]. Their molecular weights were confirmed by matrix-assisted laser desorption/ionization time-of-flight mass spectrometry (MALDI-TOF-MS): E22Δ-Aβ40 (*m/z*: calcd: 4201.76; found:

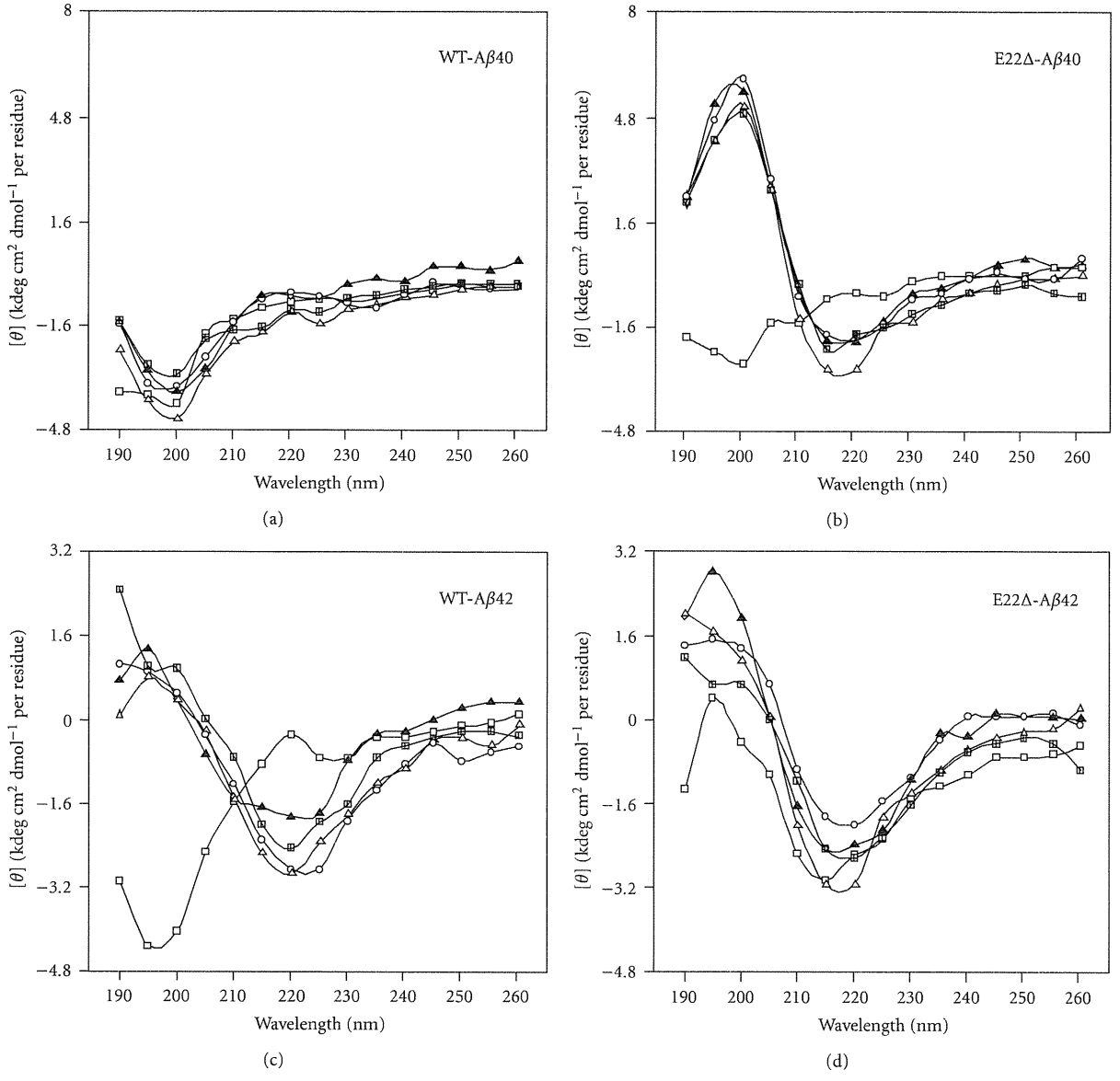

FIGURE 2: CD spectra of E22Δ-Aβ40 and E22Δ-Aβ42 (25 μM). (a) Aβ40, (b) E22Δ-Aβ40, (c) Aβ42, (d) E22Δ-Aβ42. Each Aβ (25 μM) was incubated in phosphate buffer at 37°C for the following times: □, 0 h; ▲, 4 h; △, 8 h; ∘, 24 h; ■, 48 h.

4201.56 $[M + H]^+$), E22Δ-Aβ42 (*m/z*: calcd: 4386.00; found: 4385.98 $[M + H]^+$).

2.2. Sedimentation Assay. The aggregation kinetics of each Aβ (25 μM) was estimated with the sedimentation assay using HPLC. The experimental procedure was described elsewhere [13]. The area of absorption at 220 nm was integrated and expressed as a percentage of the control.

2.3. Thioflavin T (Th-T) Fluorescence Assay. Aggregative ability of each Aβ (25 μM) was evaluated by the Th-T method developed by Naiki and Gejyo [17]. The measurement was performed on a Multidetection Microplate Reader powerscan HT (Dainippon Sumitomo Pharma) at room temperature, as described elsewhere [13]. Fluorescence intensity was measured at 450 nm excitation and 482 nm emission.

2.4. Western Blotting. Gel electrophoresis using 10–20% Tricine gel (Invitrogen, Carlsbad, CA) and Western blots analysis were carried out according to the manufacturer's protocol. The experimental procedure was described elsewhere [12]. Briefly, each Aβ was dissolved in 0.1% NH_4OH at 250 μM. After a 10-fold dilution by 50 mM sodium phosphate containing 100 mM NaCl at pH 7.4, the resultant peptide solution (25 μM) was incubated for 0, 2, or 4 hr at

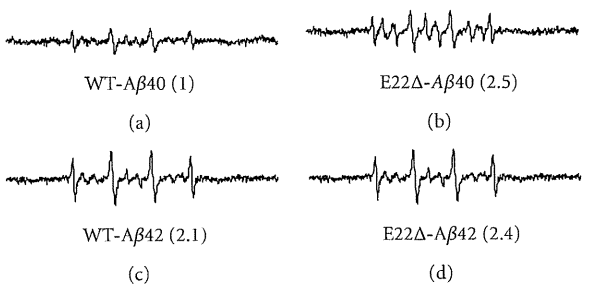

FIGURE 3: ESR spectra of E22Δ-Aβ40 and E22Δ-Aβ42 (100 μM) after 48-hr incubation at 37°C. (a) Aβ40, (b) E22Δ-Aβ40, (c) Aβ42, (d) E22Δ-Aβ42. The spectra of Aβ are shown after subtraction of the background spectrum in the presence of PBN without Aβ. Numbers in parentheses represent relative integral intensities of ESR signals, where the intensity of Aβ40 was taken as 1.0.

37°C. The anti-N-terminus of Aβ antibody, 82E1, (Immuno-Biological Laboratories Co., Ltd., Gunma, Japan) was used at 1 μg/mL as the primary antibody.

2.5. CD Spectrometry. Each Aβ was dissolved in 0.1% NH_4OH at 250 μM and diluted 10 times with 50 mM phosphate buffer (pH 7.12). The procedure was described elsewhere [16].

2.6. ESR Spectrometry. A reliable method for estimating the ability of Aβ (100 μM) to produce radicals using ESR was developed by Butterfield's group [18]. ESR spectrometry was performed on an EMX ESR spectrometer (Bruker BioSpin K.K., Karlsruhe, Germany) at room temperature, as described elsewhere [19].

2.7. Estimation of Cell Survival. To evaluate the neurotoxicity of Aβ using an MTT assay, we used undifferentiated PC12 cells, which have the potential to differentiate into neural cells, are sensitive to Aβ, and are generally used for detecting neurotoxicity as a neurotoxicity model [20]. The experimental procedure was described elsewhere [15].

2.8. Preparation of Primary Culture and Estimation of Cell Survival. Near-pure neuronal cultures were obtained from the cerebral cortices of fetal rats (17–19 days of gestation) as described [21, 22]. Cultures were maintained in Eagle's MEM supplemented with 10% heat-inactivated fetal bovine serum or 10% heat-inactivated horse serum at 37°C in a humidified 5% CO_2 atmosphere. To prevent the proliferation of nonneural cells, 10 μM cytosine β-arabinofuranoside hydrochloride was added after 5 days of plating. In all experiments mature cells used after 11–13 days *in vitro*. Animals were treated in accordance with the guidelines of the Kyoto University animal experimentation committee and the guidelines of the Japanese Pharmacological Society.

Each Aβ was dissolved in 0.02% NH_4OH at 200 μM and diluted on ice immediately before treatment. After 48 hr treatment, neurotoxicity was evaluated by lactate dehydrogenase (LDH) release assay and MTT assay.

2.9. Long-Term Potentiation. Field excitatory postsynaptic potentials (fEPSPs) were recorded from the CA1 region of rat hippocampal slices (Wistar rats, male, 6 weeks old) by electrically stimulating the Schaffer collateral [23]. Hippocampal slices were soaked in E22Δ-Aβ40, E22Δ-Aβ42, and E22P-Aβ42 solution [20 μg/200 mL phosphate-buffered saline (PBS)] before high-frequency stimulation (5 trains consisted of four 100-Hz pulses with an intertrain interval of 200 ms). fEPSPs were measured in the presence and absence of each Aβ.

3. Results and Discussion

3.1. Aggregative Ability of E22Δ Mutants. E22Δ-Aβ40 and E22Δ-Aβ42 were examined for their aggregative ability by a sedimentation assay: HPLC analysis after centrifugation of each Aβ solution. Both E22Δ-Aβ40 and E22Δ-Aβ42 aggregated at a velocity similar to Aβ42, while Aβ40 hardly aggregated even after 24-hr incubation (Figure 1(a)). This suggests that the ability to form aggregates of both E22Δ-Aβ40 and E22Δ-Aβ42 would be comparable to that of Aβ42 though soluble Aβ assemblies (oligomers) could not be distinguished from high-molecular weight fibrils in this assay condition (centrifugation: 20,000 g × 10 min). In the Th-T assay, which can estimate the β-sheet structure in Aβ aggregates [17], E22Δ-Aβ40 showed higher fluorescence than Aβ40. In contrast, the maximum fluorescence of E22Δ-Aβ42 did not exceed that of Aβ42, although the velocity of E22Δ-Aβ42 showing fluorescence was slightly higher than that of Aβ42 (Figure 1(b)). These data suggest that the E22Δ mutation accelerates the aggregation of Aβ.

Western blotting was carried out to estimate accurately the oligomerization state of Aβ. E22Δ-Aβ42 formed trimers exclusively, but E22Δ-Aβ40 produced dimers immediately after incubation (Figure 1(c)), as did the cases in the paper by Tomiyama et al. [14]; however, our Th-T assay results do not coincide with their results [14]; under Tomiyama's conditions, both mutants showed almost no fluorescence, even after 7 days. This discrepancy of the Th-T test may be due to the different conditions to make aggregates, presumably resulting in the generation of oligomers containing a β-sheet structure, as Ishii and coworkers suggested [24, 25].

3.2. Secondary Structure of E22Δ Mutants. To investigate the secondary structure of E22Δ-Aβ40 and E22Δ-Aβ42, their CD spectra were measured. In the control experiment using Aβ42 (Figure 2(c)), the positive peak at 200 nm and the negative peak at 220 nm gradually increased during the 48-hr incubation, suggesting that transformation of the random organization into a β-sheet structure occurred, while Aβ40 remained mainly random (Figure 2(a)). In contrast, E22Δ-Aβ42 formed a β-sheet-rich structure immediately after dissolution (Figure 2(d)). The velocity of the transformation of E22Δ-Aβ40 was also higher than that of Aβ42 (Figure 2(b)).

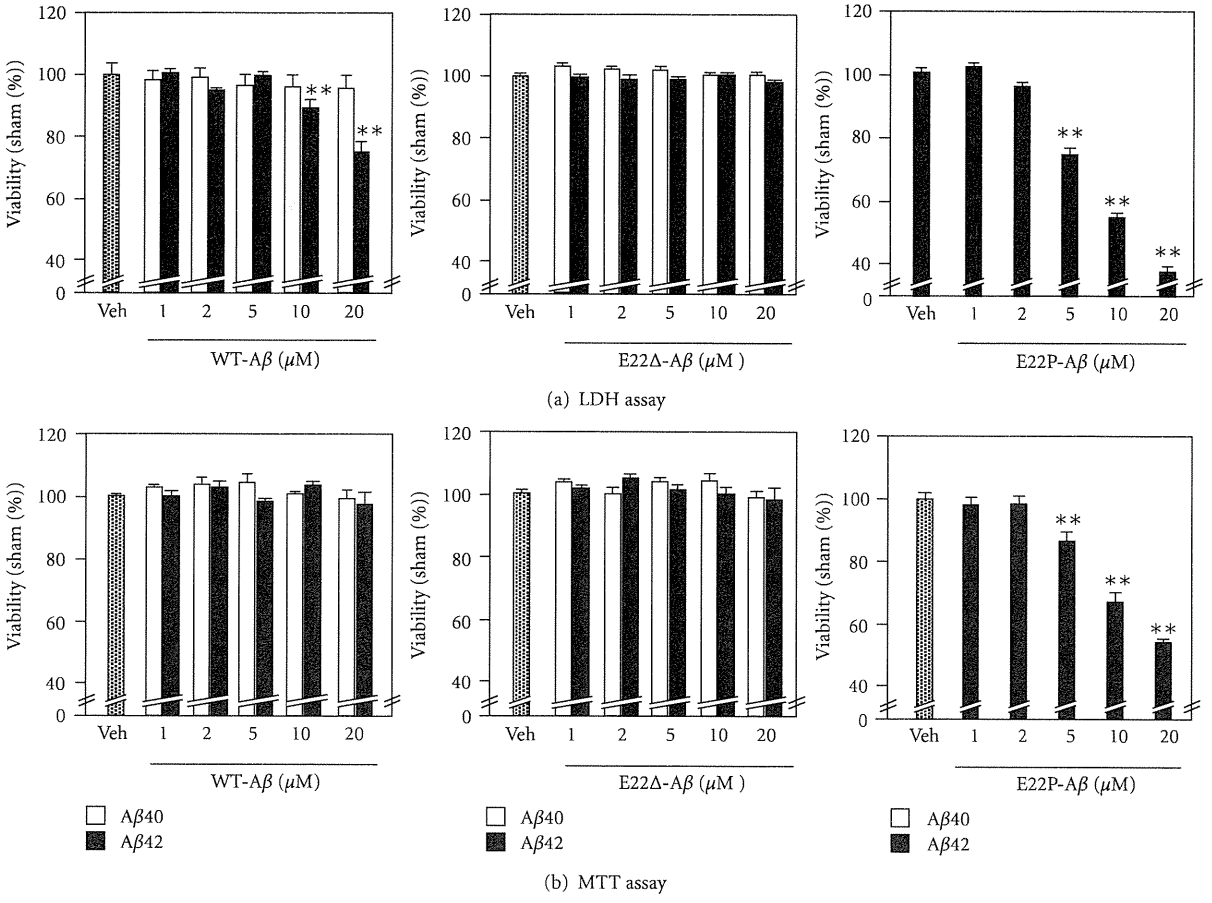

FIGURE 4: Neurotoxicity of Aβ40, Aβ42, E22Δ-Aβ40, E22Δ-Aβ42, and E22P-Aβ42 with the indicated concentration (1, 2, 5, 10, and 20 μM) using primary rat cortical neuronal cell cultures after 48-hr incubation at 37°C. Data are expressed as the mean ± s.e.m. $*P < .05$ *versus* vehicle, $**P < .01$ *versus* vehicle. Veh: vehicle.

These results suggest that the E22Δ mutation induces β-sheet transformation to form Aβ oligomers under our condition.

3.3. Radical Production by E22Δ Mutants. Our previous studies suggested that the radical productivity of Aβ42 mutants at position 22 such as E22P-, E22K-, E22Q-, and E22G-Aβ42 correlated with their aggregative ability and neurotoxicity [7]. To investigate the effect of E22Δ mutation in Aβs on the radical-generating activity, ESR was measured using phenyl-*N*-*tert*-butylnitrone (PBN) as a spin-trapping reagent (Figure 3). ESR signals of E22Δ-Aβ40 were twice more potent than those of Aβ40, and E22Δ-Aβ42 also showed slightly stronger signals than Aβ42. The radical productivity of the E22Δ-Aβs correlated basically with their ability to form oligomers and a β-sheet structure (Figures 1(c), 2).

3.4. Neurotoxicity of E22Δ-Aβs in Primary Rat Cortical Neuronal Cell Cultures. Having demonstrated that E22Δ mutation enhanced the β-sheet structure and radical productivity, we assessed the effect of this mutation on the neurotoxicity in primary rat cortical neuronal cell cultures by LDH and MTT assay (Figure 4). Treatment of the neurons with 1–20 μM of wild-type Aβ42 for 2 days induced neurotoxicity in a dose-dependent manner in the LDH test (Figure 4(a), left), in which the released LDH of the damaged cells (mainly neurons) was measured in the medium. E22P-Aβ42 with a turn at positions 22, and 23 induced stronger damage to the neurons than wild-type Aβ42; cell viability was less 40% at 20 μM (Figure 4(a), right). On the other hand, the difference in cell viability between the vehicle and wild-type Aβ42 did not reach a significant level in the MTT assay even at 20 μM (Figure 4(b), left). The cell viability of E22P-Aβ42 in MTT was also about 50% at 20 μM. In the MTT assay, total cells containing neurons, astrocytes, and microglia damaged by Aβs were counted. Since the neurons are more sensitive to damage than astrocytes or microglia in the primary cell cultures [26], the "neurotoxicity" estimated by the LDH test is often stronger than that evaluated by the MTT test.

It is worth noting that E22Δ-Aβ40 and E22Δ-Aβ42 as well as Aβ40 at 20 μM failed to show neurotoxicity against the primary cultures both in the LDH and MTT tests (Figure 4). These results are consistent with those reported by Takuma

et al.; the neurotoxicity of E22Δ-Aβ42 was very weak against mouse neuroblastoma Neuro-2a and human neuroblastoma IMR-32 [15]. In our MTT test using rat neuroblastoma PC12 cells, the IC_{50} of E22Δ-Aβ42 and wild-type Aβ42 was $4.6 \pm 1.1\,\mu M$ and $0.65 \pm 0.11\,\mu M$, respectively, showing that E22Δ-Aβ42 was significantly less toxic than wild-type Aβ42. The neurotoxicity of E22Δ-Aβ40 ($IC_{50} = 10 \pm 1.0\,\mu M$) was weak as expected, but slightly stronger than that of Aβ40 ($IC_{50} = 20 \pm 1.0\,\mu M$).

3.5. Synaptotoxicity of E22Δ Mutants. Selkoe and coworkers suggested that Aβ dimers are the smallest synaptotoxic species inhibiting the LTP in the pathogenesis of AD and that plaque cores are largely inactive but sequester and release dimers [27]. Tomiyama et al. reported the more potent inhibition of LTP by E22Δ-Aβ42 than by wild-type Aβ42 [14]. We tested the inhibition of LTP by E22Δ-Aβ40 using rat hippocampal slices. Figure 5 shows that E22Δ-Aβ40 is not such a potent inhibitor of LTP as E22Δ-Aβ42, whose inhibitory potency was stronger that of than wild-type Aβ42, as Tomiyama et al. reported [14]. This coincides with the previous datas that the 42-mer Aβ showed more potent neurotoxicity than 40-mer Aβ [13]. Notably, E22P-Aβ42, which can more readily form a toxic conformer with a turn at positions 22 and 23 than wild-type Aβ42 [11], inhibited the LTP more strongly than E22Δ-Aβ42 at an almost undetectable level after 60 min (Figure 5(b)). This suggests that the conformation at positions 22 and 23 of E22P-Aβ42 might be similar to that of E22Δ-Aβ42 at positions 21 and 23.

3.6. Relevance of E22Δ Mutation to Turn-Induced Neurotoxicity. The present results suggest that E22Δ mutation in Aβ accelerates the transformation of a random form into a β-sheet structure (Figure 2) and radical productivity (Figure 3) but does not increase neurotoxicity in primary rat cortical neuronal cell cultures (Figure 4). E22Δ-Aβ42 synthesized in our laboratory showed the significant formation of oligomers (Figure 1) and synaptotoxicity (Figure 5), as reported by Mori and coworkers [14]. In addition, E22P-Aβ42 inhibited LTP more severely than E22Δ-Aβ42 (Figure 5). We previously reported that E22P-Aβ42, with a turn at positions 22 and 23 as a Pro-X corner (X: variable amino acid residue) [28], could form significant oligomers [11] with a β-sheet-rich structure [16] and radicals to result in potent neurotoxicity with the formation of radicals [7]; therefore, E22Δ-induced synaptotoxicity might be in part related to turn-induced radical formation. This implies that conformational change in E22Δ-Aβ is similar to that in E22P-Aβ42, but is not the same since E22Δ-Aβ42 exhibited no neurotoxicity, unlike E22P-Aβ42 and wild-type Aβ42.

It should be noted that the effects of E22Δ mutation on the physicochemical properties of Aβ40 are significantly higher than those of Aβ42. This tendency is similar to cases of other CAA or FAD mutant Aβs. We previously reported a comprehensive study on the aggregation, neurotoxicity, and secondary structure of Aβ mutants at positions 21–23 (A21G, E22G, E22Q, E22K, and D23N) [13]. Since Aβ40

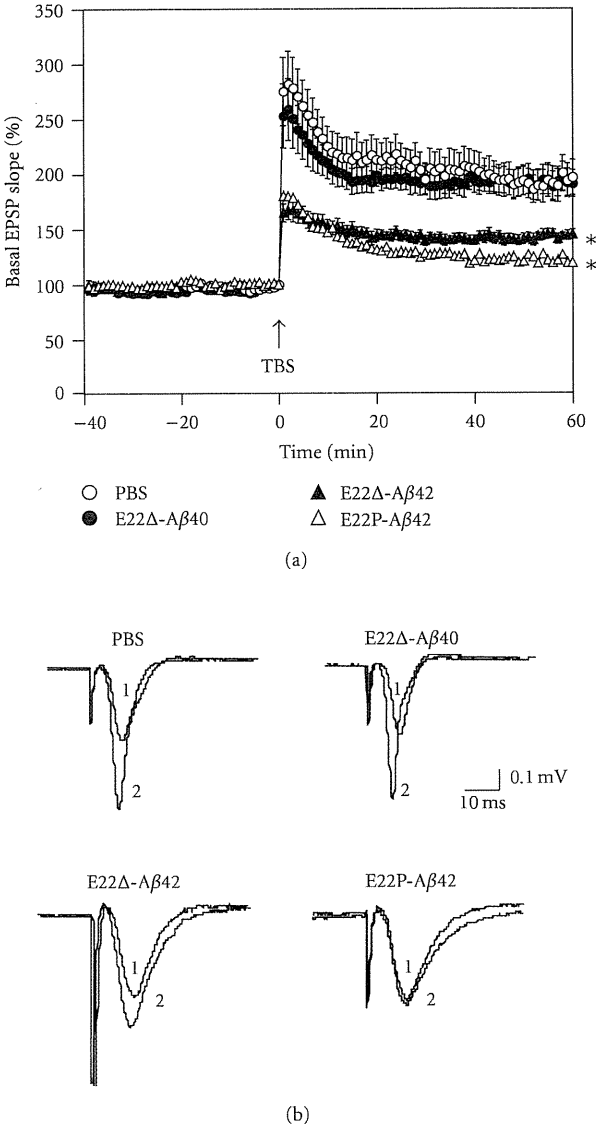

FIGURE 5: *In vivo* synaptotoxicity of E22Δ-Aβ40, E22Δ-Aβ42, and E22P-Aβ42 estimated by LTP expression. (a) Field excitatory postsynaptic potentials (fEPSPs) were recorded from the CA1 region of rat hippocampal slices (Wistar rats, male, 6 weeks old) by delivering theta burst stimulation (TBS) to the Schaffer collateral/commissural pathway. LTP was induced by high-frequency stimulation (5 trains consisted of four 100-Hz pulses with an intertrain interval of 200 ms) in the presence and absence of each Aβ (20 μg/200 mL PBS), to be injected into the lateral ventricle 20 min before stimulation. Each point on the graph represents the mean ± s.e.m. of basal fEPSP slope (0 min); $n = 12$ for PBS, $n = 9$ for E22Δ-Aβ40, $n = 10$ for E22Δ-Aβ42, and $n = 10$ for E22P-Aβ40. $^*P < .0001$ versus PBS; $P = .4258$ between PBS and E22Δ-Aβ40. $P < .0001$ versus PBS, when fEPSP slopes were compared with 1 to 60 min after TBS. The means between the four groups were compared using analysis of variance followed by Fisher's protected least significant difference (PLSD) test. ○, PBS; ●, E22Δ-Aβ40; ▲, E22Δ-Aβ42; △, E22P-Aβ42. (b) Typical field excitatory postsynaptic potentials at (1) 0 and (2) 60 minutes after TBS.

is secreted in neurons about nine times more abundantly than Aβ42 [3], in some cases Aβ40 may play a critical role in the pathogenesis of CAA or FAD. In addition, the E22Δ mutant of Aβ40 [14] as well as the CAA- or FAD-related Aβ40 mutants at positions 21, 22, and 23 have been reported to be more resistant than wild-type Aβ40 against degradation by insulin-degrading enzyme [29]; however, it remains controversial whether E22Δ is a familial type of AD or AD-type dementia.

Mori, Tomiyama, and coworkers implied the intracellular accumulation of Aβ oligomers using cultured cells [30] and their own developed mouse model [31] with E22Δ mutation. This mutation also caused apoptosis induced by stress in the endoplasmic reticulum [30]. Quite recently, we proposed the involvement of a turn at positions 22 and 23 of Aβ in intracellular amyloidosis [32]. Thus, the increase of radical productivity by E22Δ mutation is in good agreement with the turn-induced oxidative stress of Aβ42 [7], presumably *via* the interplay between Tyr10 and Met35 [12]. The deletion mutation of the residue at position 22 might promote Tyr10 in close proximity to the sulfur atom of Met35, inducing the effective production of radicals.

4. Conclusion

In summary, E22Δ-Aβ42 effectively induced the transformation of a random form to a β-sheet structure and the formation of radicals accompanied with oligomerization. However, the molecular mechanism of the pathology of AD of E22Δ-Aβ42 might be different from that of wild-type Aβ42 since E22Δ-Aβ42 showed more potent synaptotoxicity but weaker neurotoxicity than wild-type Aβ42.

Acknowledgments

The authors thank Dr. Hiroyuki Fukuda at the Institute of Medical Science, The University of Tokyo for MALDI-TOF-MS measurements, and Drs. Noriaki Kinoshita and Yuko Horikoshi-Sakuraba at Immuno-Biological Laboratories Co., Ltd. for providing the antibody 82E1. This research was supported in part by grants-in-aid for Scientific Research (A) (Grant no. 21248015 to K.I.) and Scientific Research (C) (Grant no. 22603006 to K.M.) from the Ministry of Education, Culture, Sports, Science and Technology of the Japanese Government and in part by the Alzheimer's Association (IIRG-09-132098) to HM.

References

[1] G. G. Glenner and C. W. Wong, "Alzheimer's disease: initial report of the purification and characterization of a novel cerebrovascular amyloid protein," *Biochemical and Biophysical Research Communications*, vol. 120, no. 3, pp. 885–890, 1984.

[2] C. L. Masters, G. Simms, and N. A. Weinman, "Amyloid plaque core protein in Alzheimer disease and Down syndrome," *Proceedings of the National Academy of Sciences of the United States of America*, vol. 82, no. 12, pp. 4245–4249, 1985.

[3] C. Haass and D. J. Selkoe, "Soluble protein oligomers in neurodegeneration: lessons from the Alzheimer's amyloid β-peptide," *Nature Reviews Molecular Cell Biology*, vol. 8, no. 2, pp. 101–112, 2007.

[4] C. Behl, J. B. Davis, R. Lesley, and D. Schubert, "Hydrogen peroxide mediates amyloid β protein toxicity," *Cell*, vol. 77, no. 6, pp. 817–827, 1994.

[5] D. A. Butterfield, "Amyloid β-peptide [1–42]-assosiated free radical-induced oxidative stress and neurodegeneration in Alzheimer's disease brain: mechanisms and consequences," *Current Medicinal Chemistry*, vol. 10, no. 24, pp. 2651–2659, 2003.

[6] K. J. Barnham, C. L. Masters, and A. I. Bush, "Neurodegenerative diseases and oxidatives stress," *Nature Reviews Drug Discovery*, vol. 3, no. 3, pp. 205–214, 2004.

[7] K. Murakami, K. Irie, H. Ohigashi et al., "Formation and stabilization model of the 42-mer Aβ radical: implications for the long-lasting oxidative stress in Alzheimer's disease," *Journal of the American Chemical Society*, vol. 127, no. 43, pp. 15168–15174, 2005.

[8] K. Murakami, Y. Masuda, T. Shirasawa, T. Shimizu, and K. Irie, "The turn formation at positions 22 and 23 in the 42-mer amyloid β peptide: the emerging role in the pathogenesis of Alzheimer's disease," *Geriatrics and Gerontology International*, vol. 10, supplement 1, pp. S169–S179, 2010.

[9] D. M. Walsh, I. Klyubin, J. V. Fadeeva et al., "Naturally secreted oligomers of amyloid β protein potently inhibit hippocampal long-term potentiation in vivo," *Nature*, vol. 416, no. 6880, pp. 535–539, 2002.

[10] R. Roychaudhuri, M. Yang, M. M. Hoshi, and D. B. Teplow, "Amyloid β-protein assembly and Alzheimer disease," *Journal of Biological Chemistry*, vol. 284, no. 8, pp. 4749–4753, 2009.

[11] Y. Masuda, S. Uemura, R. Ohashi et al., "Identification of physiological and toxic conformations in Aβ42 aggregates," *ChemBioChem*, vol. 10, no. 2, pp. 287–295, 2009.

[12] K. Murakami, H. Hara, Y. Masuda, H. Ohigashi, and K. Irie, "Distance measurement between Tyr10 and Met35 in amyloid beta by site-directed spin-labeling ESR spectroscopy: implications for the stronger neurotoxicity of Aβ42 than Aβ40," *Chembiochem*, vol. 8, no. 18, pp. 2308–2314, 2007.

[13] K. Murakami, K. Irie, A. Morimoto et al., "Neurotoxicity and physicochemical properties of Aβ mutant peptides from cerebral amyloid angiopathy: implication for the pathogenesis of cerebral amyloid angiopathy and Alzheimer's disease," *Journal of Biological Chemistry*, vol. 278, no. 46, pp. 46179–46187, 2003.

[14] T. Tomiyama, T. Nagata, H. Shimada et al., "A new amyloid β variant favoring oligomerization in Alzheimer's-type dementia," *Annals of Neurology*, vol. 63, no. 3, pp. 377–387, 2008.

[15] H. Takuma, R. Teraoka, H. Mori, and T. Tomiyama, "Amyloid-β E22Δ variant induces synaptic alteration in mouse hippocampal slices," *NeuroReport*, vol. 19, no. 6, pp. 615–619, 2008.

[16] K. Murakami, K. Irie, A. Morimoto et al., "Synthesis, aggregation, neurotoxicity, and secondary structure of various Aβ1–42 mutants of familial Alzheimer's disease at positions 21–23," *Biochemical and Biophysical Research Communications*, vol. 294, no. 1, pp. 5–10, 2002.

[17] H. Naiki and F. Gejyo, "Kinetic analysis of amyloid fibril formation," *Methods in Enzymology*, vol. 309, pp. 305–318, 1999.

[18] S. Varadarajan, J. Kanski, M. Aksenova, C. Lauderback, and D. A. Butterfield, "Different mechanisms of oxidative stress and neurotoxicity for Alzheimer's Aβ(1–42) and Aβ(25–35),"

Journal of the American Chemical Society, vol. 123, no. 24, pp. 5625–5631, 2001.

[19] K. Murakami, M. Uno, Y. Masuda, T. Shimizu, T. Shirasawa, and K. Irie, "Isomerization and/or racemization at Asp23 of Aβ42 do not increase its aggregative ability, neurotoxicity, and radical productivity in vitro," *Biochemical and Biophysical Research Communications*, vol. 366, no. 3, pp. 745–751, 2008.

[20] M. S. Shearman, C. I. Ragan, and L. L. Iversen, "Inhibition of PC12 cell redox activity is a specific, early indicator of the mechanism of β-amyloid-mediated cell death," *Proceedings of the National Academy of Sciences of the United States of America*, vol. 91, no. 4, pp. 1470–1474, 1994.

[21] T. Kume, H. Kouchiyama, S. Kaneko et al., "BDNF prevents NO mediated glutamate cytotoxicity in cultured cortical neurons," *Brain Research*, vol. 756, no. 1-2, pp. 200–204, 1997.

[22] T. Kume, H. Nishikawa, H. Tomioka et al., "p75-mediated neuroprotection by NGF against glutamate cytotoxicity in cortical cultures," *Brain Research*, vol. 852, no. 2, pp. 279–289, 2000.

[23] T. Nishizaki, T. Nomura, T. Matuoka et al., "The anti-dementia drug nefiracetam facilitates hippocampal synaptic transmission by functionally targeting presynaptic nicotinic ACh receptors," *Molecular Brain Research*, vol. 80, no. 1, pp. 53–62, 2000.

[24] S. Chimon and Y. Ishii, "Capturing intermediate structures of Alzheimer's β-amyloid, Aβ(1–40), by solid-state NMR spectroscopy," *Journal of the American Chemical Society*, vol. 127, no. 39, pp. 13472–13473, 2005.

[25] S. Chimon, M. A. Shaibat, C. R. Jones, D. C. Calero, B. Aizezi, and Y. Ishii, "Evidence of fibril-like β-sheet structures in a neurotoxic amyloid intermediate of Alzheimer's β-amyloid," *Nature Structural and Molecular Biology*, vol. 14, no. 12, pp. 1157–1164, 2007.

[26] M. R. Vargas and J. A. Johnson, "The Nrf2-ARE cytoprotective pathway in astrocytes," *Expert reviews in molecular medicine*, vol. 11, p. e17, 2009.

[27] G. M. Shankar, S. Li, T. H. Mehta et al., "Amyloid-β protein dimers isolated directly from Alzheimer's brains impair synaptic plasticity and memory," *Nature Medicine*, vol. 14, no. 8, pp. 837–842, 2008.

[28] P. Y. Chou and G. D. Fasman, "β-Turns in proteins," *Journal of Molecular Biology*, vol. 115, no. 2, pp. 135–175, 1977.

[29] L. Morelli, R. Llovera, S. A. Gonzalez et al., "Differential degradation of amyloid β genetic variants associated with hereditary dementia or stroke by insulin-degrading enzyme," *Journal of Biological Chemistry*, vol. 278, no. 26, pp. 23221–23226, 2003.

[30] K. Nishitsuji, T. Tomiyama, K. Ishibashi et al., "The E693Δ mutation in amyloid precursor protein increases intracellular accumulation of amyloid β oligomers and causes endoplasmic reticulum stress-induced apoptosis in cultured cells," *American Journal of Pathology*, vol. 174, no. 3, pp. 957–969, 2009.

[31] T. Tomiyama, S. Matsuyama, H. Iso et al., "A mouse model of amyloid β oligomers: their contribution to synaptic alteration, abnormal tau phosphorylation, glial activation, and neuronal loss in vivo," *Journal of Neuroscience*, vol. 30, no. 14, pp. 4845–4856, 2010.

[32] K. Murakami, Y. Horikoshi-Sakuraba, N. Murata et al., "Monoclonal antibody against the turn of the 42-residue amyloid beta protein at positions 22 and 23," *ACS Chemical Neuroscience*, vol. 1, no. 11, pp. 747–756, 2010.